LANGMUIR

pubs.acs.org/Langmuir Article

Structure–Property Relationship in Capillary Foams

Omotola Okesanjo, J. Carson Meredith,* and Sven H. Behrens*

Cite This: *Langmuir* 2021, 37, 10510–10520 Read Online

ACCESS | Metrics & More | Article Recommendations | Supporting Information

ABSTRACT: The recently discovered capillary foams are aqueous foams stabilized by the synergistic action of colloidal particles and a small amount of oil. Characteristically, their gas bubbles are coated by a particle-stabilized layer of oil and embedded in a gel network of oil-bridged particles. This unique foam architecture offers opportunities for engineering new foam-related materials and processes, but the necessary understanding of its structure–property relations is still in its infancy. Here, we study the effects of particle wettability, particle volume fraction, and oil-to-particle ratio on the structure and selected properties of capillary foams and use our findings to relate measured foamability, foam stability, and rheological key parameters to the observed foam microstructure. We see that particle wettability not only determines the type of gel network formed but also influences the prevalence of oil droplets included within the foam. Our results further show that the stability and rheology of capillary foams are mainly a function of the particle volume fraction whereas the foamability and observed microstructure are sensitive also to the oil-to-particle ratio. These insights expand our fundamental understanding of capillary foams and will greatly facilitate future work on new foam formulations.

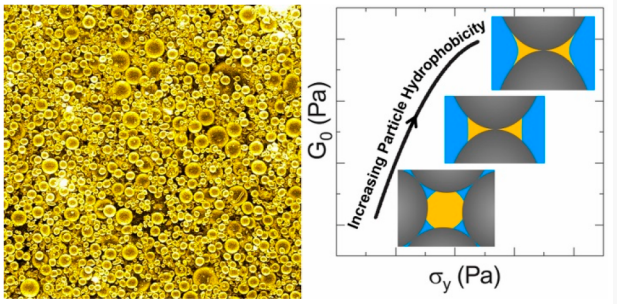

1. INTRODUCTION

Ternary systems composed of fluid/fluid/particle mixtures display different types of structures that are determined by the constituent volume fractions and wetting behavior.[1−3] Pickering emulsions, liquid marbles, and bijels are examples of different ternary states obtainable when particles interact at fluid–fluid interfaces.[4−6] Understanding the nature and properties of ternary colloidal multiphase systems plays a big role in material design and processing in the ceramics, food, pharmaceutical, and cosmetics industries. In many of the ternary fluid/fluid/particle systems, capillary interactions and particle wettability also play a major role in determining and stabilizing the observed structure.[2,7] Recently, Velankar categorized the obtainable morphologies of fluid/fluid/particle mixtures in a state diagram as a function of mixture composition and particle wettability.[8] Many of these ternary systems are composed of immiscible fluids, usually water, a water-immiscible solvent ("oil") or air, and solid particles of different surface characteristics, but liquid phases formed by immiscible polymer melts are also of interest and allow for convenient structure analysis after solidification.[3]

Ramsden and Pickering first reported in the early 20th century that particles with appropriate wettability can stabilize fluid interfaces.[9,10] Since then, it has been well-understood that colloidal particles, in the absence of insurmountable kinetic barriers, tend to adsorb irreversibly to fluid interfaces, provided that the particle wettability does not favor one fluid over the other to an extreme degree. This is because the minimum energy ΔE required to remove a single adsorbed particle of size R from the interface of two fluids with interfacial tension γ is given approximately by

$$\Delta E = \pi R^2 \gamma (1 - |\cos \theta|)^2 \quad (1)$$

where θ is the contact angle between the fluid interface and the particle surface, and typical values of ΔE exceed the thermal energy scale, kT, by orders of magnitude. Both interfacial tension and particle wettability, for which θ is a measure, are important in the formation and stability of ternary systems; however, the particle wettability has a stronger influence on the system morphology. The values of θ in ternary systems range between 0° to 180°, where both extremes indicate complete wetting of the particles by one of the two fluids. Much attention has been given to systems stabilized by particles with near-neutral wetting (θ close to 90°).[11−13] More recently, work has been devoted to understanding ternary systems in which one fluid preferentially wets the particles, which commonly occurs *e.g.* in capillary suspensions.[14]

Capillary suspensions are particle suspensions that include a small amount of an immiscible secondary liquid. The addition of the secondary liquid and mixing leads to the formation of a space spanning network of particles bridged by the secondary

Received: June 2, 2021
Revised: August 3, 2021
Published: August 26, 2021

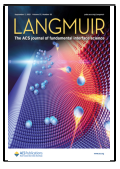

https://doi.org/10.1021/acs.langmuir.1c01479
Langmuir 2021, 37, 10510–10520

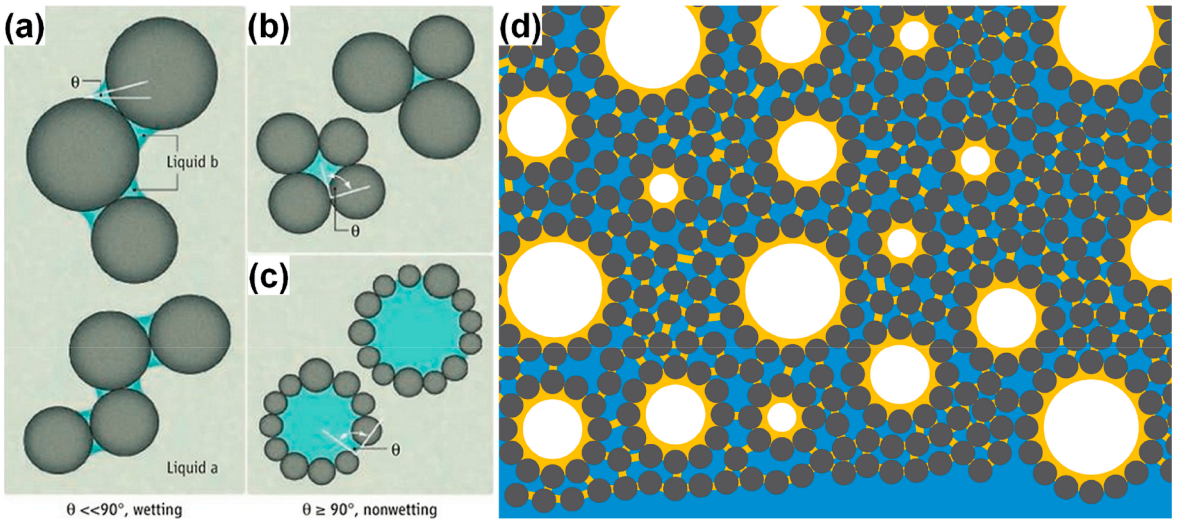

Figure 1. Schematic showing how secondary liquids interact with particles by formation of (a) pendular bridges, (b) capillary aggregates, or (c) droplet stabilized by particles (Reprinted with permission from ref 15. Copyright 2011 AAAS). (d) Schematic of capillary foams showing the oil-coated bubbles and the oil-bridged particle network (not to scale).

liquid.[16] The type of bridging between the particles is determined by the wettability of the particles toward the primary and secondary liquids.[15] When the secondary liquid wets the particles preferentially, it forms pendular bridges between particles in a network structure referred to as the pendular state (see Figure 1a). When the continuous fluid medium wets the particles preferentially, the secondary liquid forms polydisperse bridges each of which typically connect several particles and which together stabilize a network of particle aggregates in the so-called capillary state (see Figure 1b).[17] Either type of network tends to propagate beyond the percolation threshold and causes the system to gel.[18,19] The differences between the modulus and yield stress in capillary suspensions and the neat suspension (without the secondary liquid) extend over multiple orders of magnitude because of the strong capillary force that holds the particles together. Capillary interactions also play a crucial role in a closely related class of foams called capillary foams.[20]

Capillary foams (CFs) are formed in water and stabilized by the synergistic action of particles and a small amount of secondary immiscible liquid (oil) that mediates capillary interactions.[20,21] CFs contain gas bubbles that are coated by a composite layer of oil and particles and enclosed within a gel network of a capillary suspension that represents the continuous phase of the foam (see Figure 1d). The formation of CFs has been attributed to particle assisted spreading of oil around the air−water interface[20] and subsequent entrapment of the coated bubbles in the nascent capillary network formed under mechanical agitation.[22] For many readily water-dispersible particles, this new foam class has been observed to offer better long-term stability than its (oil-free) Pickering foam counterpart.[20] The unique architecture in CFs significantly impacts foam properties. For example, CF rheology was found to be similar to the rheology of surfactant foams that have high gas volume fractions, despite the fact that CFs have low gas volume fractions ($0.2 < \phi_g < 0.45$). Rheological studies also showed that CFs have relatively high viscosities and are shear thinning after yielding.[23] Other experiments have also shown that the added oil enables functionalization of CFs through oil-phase additives that add a degree of versatility not known from other aqueous foams.[24] The interesting mechanical properties and tunability of CFs allow for the possibility of engineering new foam based products for commercial and industrial use.

CFs, having three, not two, immiscible fluids are a separate class of mixtures from those discussed above; they are distinct and are not represented in Velankar's prism of ternary mixtures.[8] Given that the addition of a secondary immiscible liquid to a suspension has significant structural and rheological implications, the introduction of a third immiscible fluid can be expected to induce unprecedented changes to a ternary system mixture. Indeed, the constituent elements of CFs, including bubbles, oil, water, and particles, all come together to establish the unique properties that have been observed in CFs. While the effects of the type and concentration of oil and particles on the foamability and stability of CFs have been qualitatively characterized from a macroscopic perspective, a major question that has not been answered in the literature is how the CF composition and the particle wettability affect the structure and mechanical properties of CFs.[22] Given the uniqueness of CFs, the answer to this question cannot easily be obtained or extrapolated from the results of the previous work on ternary systems. Nevertheless, it is important to understand how CF morphology and rheology vary with its constituent ratios and wettability because the answer to this question will not only provide fundamental understanding of multiphase quaternary systems and how they differ from ternary systems but will also dictate how CFs can be engineered for use in various products and processes.

In this paper, we study the influence of constituent variations on the microstructure and rheology of CFs. We vary the stoichiometry of the condensed matter components but do not control the amount of gas incorporated, because unlike the amount of secondary liquid in a capillary suspension, the gas volume fraction in CFs cannot be varied easily and directly but is determined, for a given frothing procedure, by the stoichiometry of the foam's solid and liquid components. Microscopy, rheology, and foamability experiments are carried out to determine how the particle wettability and the constituent ratios affect the rheology and microstructure in capillary foams. The observed CF microstructures and obtained rheological measurements as well as their effects on

https://doi.org/10.1021/acs.langmuir.1c01479
Langmuir 2021, 37, 10510−10520

Table 1. Properties of Particles Used in Foaming, Microscopy, and Rheology Experiments

particle identifier	particle name (supplier)	size[a] (nm)	zeta-potential[a] (mV)	emulsion formed	comments
P_1	HDK H30 (Wacker)	466 ± 27	−25.3 ± 1.3	oil-in-water	
P_2	Aerosil R 972 (Evonik)	594 ± 18	−24.6 ± 0.6	water-in-oil	
P_3	Aerosil R 812S (Evonik)	215 ± 1	−21.6 ± 0.7	water-in-oil	most hydrophobic; the only particles to allow for the production and stabilization of large (Pickering) foam volumes by frothing oil-free dispersions

[a]The uncertainty represents the standard deviation from the average value of three independent measurements.

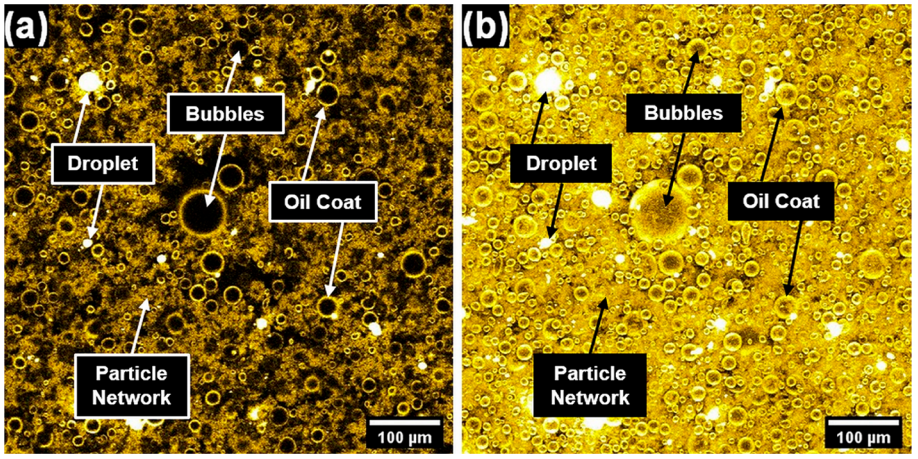

Figure 2. Confocal micrographs showing (a) single image in the $x-y$-plane of capillary foams made with P_1 at a particle volume fraction $\phi_p = 0.92\%$ and an oil−particle ratio $\varrho = 0.2$. (b) z-Stack projections of multiple images. Bright regions show the fluorescent oil.

CF properties such as foamability and foam stability are outlined and discussed in detail. Lastly, we compare our results to what has been reported on capillary suspensions and discuss the implications of these results in relation to the tuning of CF properties for potential applications.

2. EXPERIMENTAL SECTION

2.1. Materials. Amorphous fumed silica particles partially modified with dichlorodimethylsilane were provided by Wacker-Chemie AG (Germany); they retained 50% residual silanol groups on the surface according to the vendor. Two more strongly hydrophobized types of fumed silica particles were provided by Evonik (USA): Aerosil R 972, also modified by dichlorodimethylsilane, and Aerosil R 812S, modified by hexamethyldisilazane (HMDS). Trimethylolpropane trimethacrylate (TMPTMA), a photopolymerizable solvent used in several previous studies as the foam's oil component, was obtained from Sigma-Aldrich. A previous study on CFs discusses the suitability of oil−particle pairs for CF formation and shows that the combination of TMPTMA with silica particles enables the spreading of oil around the air−water interface and facilitates the formation of capillary foams.[20] Deionized water was used as the aqueous continuous phase for the CFs. All foams were prepared using a rotor-stator homogenizer (IKA Ultra-Turrax T10, rotor diameter of 6.1 mm, stator diameter 8 mm).

2.2. Particle Dispersion. Silica particles were initially dispersed in methanol. The particle solution was centrifuged, and the methanol supernatant was removed. The particle sediment was rinsed with DI-water by first resuspending the particles in DI-water, sonicating the solution to properly disperse the particles, and finally centrifuging the solution. The particles were rinsed at least five times to effectively remove the methanol.

2.3. Particle Characterization. Particle sizes and zeta potentials were determined by dynamic and electrophoretic light scattering using a Malvern Zetasizer Nano ZS90. The hydrodynamic radii and zeta-potentials of the silica particles were obtained in 5 mM sodium chloride (NaCl) solution. The relative wettability of the silica particles by the two liquid foam components was characterized qualitatively by determining their "preferred emulsion type", i.e. the type of emulsion (o/w or w/o) formed when mixing equal volumes of TMPTMA and aqueous (0.1 wt %) particle dispersion. Table 1 lists the particle properties and emulsion types stabilized by the particles used in this work.

2.4. Capillary Foam Preparation. Silica particles suspended in DI-water containing 5 mM NaCl salt were prepared in a 20 mL vial. TMPTMA was added to the silica suspension at the appropriate oil−particle ratio. CFs were prepared by mechanically frothing the mixture at 30 000 rpm for 2 min, unless otherwise mentioned.

2.5. Foam Imaging. Confocal images of capillary foams were obtained via laser scanning confocal microscopy experiments on an inverted microscope (Olympus, IX81; 60×, 20×, and 4× objectives). An oil soluble fluorescent dye (Nile red) was added to the TMPTMA oil used to prepare the capillary foams. Nile red was excited using a 546 nm laser and emission detected above 650 nm. All microscopy images were processed using ImageJ software.

2.6. Rheology Measurements. An Anton Paar MCR 501 rheometer equipped with a temperature controller was used to perform rheological measurements on the capillary foams. To prevent inaccuracies that arise from shear localization and wall-slip in our rheological measurements, we used a vane geometry tool (d = 16 mm, l = 22 mm; cup: d = 28.9 mm) in the rheology experiments.[25]

The capillary foams were prepared in the rheometer cup. The temperature was maintained at 25 °C. Once prepared, the CFs were allowed to equilibrate at rest for 10 min before the start of the steady and oscillatory shear experiments. Frequency sweep oscillatory measurements at a strain $\gamma = 0.001$ were obtained before and after each experiment to assess the state of the foam. Prior work demonstrates the reproducibility of CF rheology data.[23] Repeat measurements on independently prepared batches suggest a range of uncertainty for the rheology data comparable to the size of the markers. Figure S4 presents a sample of the original data overlaid by the replicate data obtained from a fresh CF.

https://doi.org/10.1021/acs.langmuir.1c01479
Langmuir 2021, 37, 10510−10520

3. RESULTS AND DISCUSSION

3.1. Foam Structure. The internal structure of our capillary foams was probed by detecting the fluorescence oil phase via confocal microscopy. Figure 2a is a typical confocal image showing the location of the oil in a thin slice of the capillary foam. Where the image plane cuts through the oil coat surrounding the spheroidal bubbles, bright circles with a dark center can be seen. The oil bridges connecting particles in the gel matrix are too small to be resolved individually, but they contribute to the diffuse "clouds" of brightness visible in the space outside the bubbles. Spots of intense brightness indicate oil droplets incorporated in the network as well. For a more 3-dimensional impression of the same foam sample, Figure 2b shows a "z-stack projection", i.e., the overlay of 163 two-dimensional images of the x−y-plane, such as Figure 2a, taken at different z-positions spanning 81 μm in depth. The CF imaged in this figure was prepared with P_1 particles at a particle volume fraction ϕ_p = 0.92% with respect to the total volume of the condensed phases (water + particles + oil) and at an oil−particle volume ratio ϱ = 0.2.

As Figure 2 illustrates, the network of oil-bridged particles occupies a significant portion of the capillary foam structure. The microstructure observed from the confocal micrographs reveal that bubbles in these CFs are polydisperse, with bubbles sizes ranging from a few microns to hundreds of microns in diameter. By measuring the area fraction of the bubble interior spaces in Figure 2b, we determined that the gas volume fraction ("foam quality") in this CF is ∼34%.

Apart from oil-coated bubbles and the particle network, we also observe that oil droplets are present within the CFs structure shown in the confocal micrographs in Figure 2. The presence of oil droplets in CFs is unexpected, because oil droplets were not observed in previously reported structures and images of CFs.[20,22,24] The coexistence of oil droplets and bubbles is not unique to CFs but has been observed in systems sometimes referred to as *foamulsions*,[26,27] in which all of the oil resides in droplets accumulating within the plateau borders of a denser, particle-free foam. The oil, in water-continuous foamulsions, does not engulf the bubbles, bridge solid particles, or stabilize a particle network. Furthermore, the amount of oil droplets as a fraction of the total liquid volume in foamulsions is typically higher than the entire oil per total liquid volume in a capillary foam and much higher than the volume fraction of the newly discovered droplets in some capillary foams. In capillary foam, by contrast, the oil is closely associated with the particles: particles facilitate the spreading of the oil around the bubbles and stabilize the bubble coating layer of oil, and oil bridges are anchored between particles in the gel network. We similarly assume that adsorbed particles stabilize the droplets of excess oil seen in Figure 2; after all, their high affinity for the oil−water interface and preferential wetting by the water phase should also qualify these P_1 particles as oil-in-water emulsion stabilizers (see Figure 1c and Table 1). One should then expect the occurrence and prevalence of bulk oil droplets in the CFs to be a function of the particle wettability and/or the oil−particle ratio. This hypothesis shall be explored next.

3.1.1. Effect of Oil-Particle Ratio on Capillary Foam Structure. First, we document the changes that occur in the CF microstructure as ϱ is increased in CFs prepared using P_1 particles. Figure 3a−c shows a series of confocal images of the CF structure that were obtained for an oil−particle volume ratio ϱ of 0.2, 0.5, and 1, respectively, at a fixed particle volume fraction ϕ_p = 0.92 vol %. The images in Figure 3 show that the number of droplets, visible as intense bright spots in the CFs, increases with ϱ. The number of droplets at the lowest oil−particle ratio (ϱ = 0.2) is small (Figure 3a), with typically only 1−2 droplets in a 212 μm × 212 μm field of view, whereas much of the visible oil is incorporated in the bubble coats and in the diffuse oil−particle network. At higher ϱ (Figure 3b and

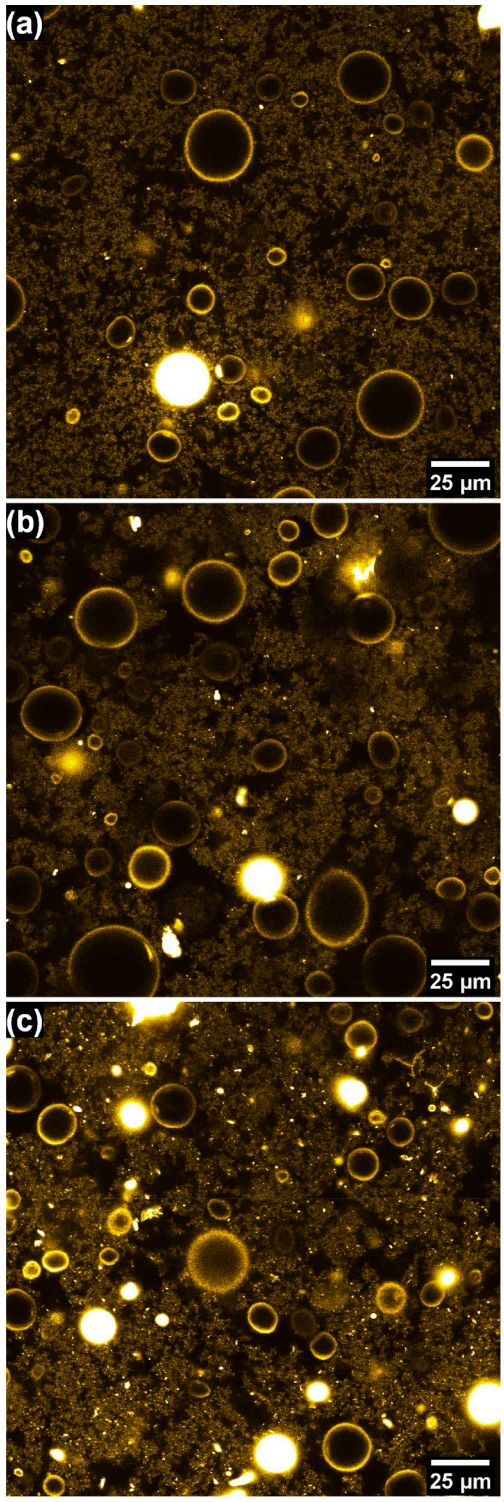

Figure 3. Confocal micrograph grid of capillary foams at different oil−particle ratios, ϱ = (a) 0.2, (b) 0.5, (c) 1, all at a constant particle volume fraction ϕ_p = 0.92% of P_1 particles.

https://doi.org/10.1021/acs.langmuir.1c01479
Langmuir 2021, 37, 10510−10520

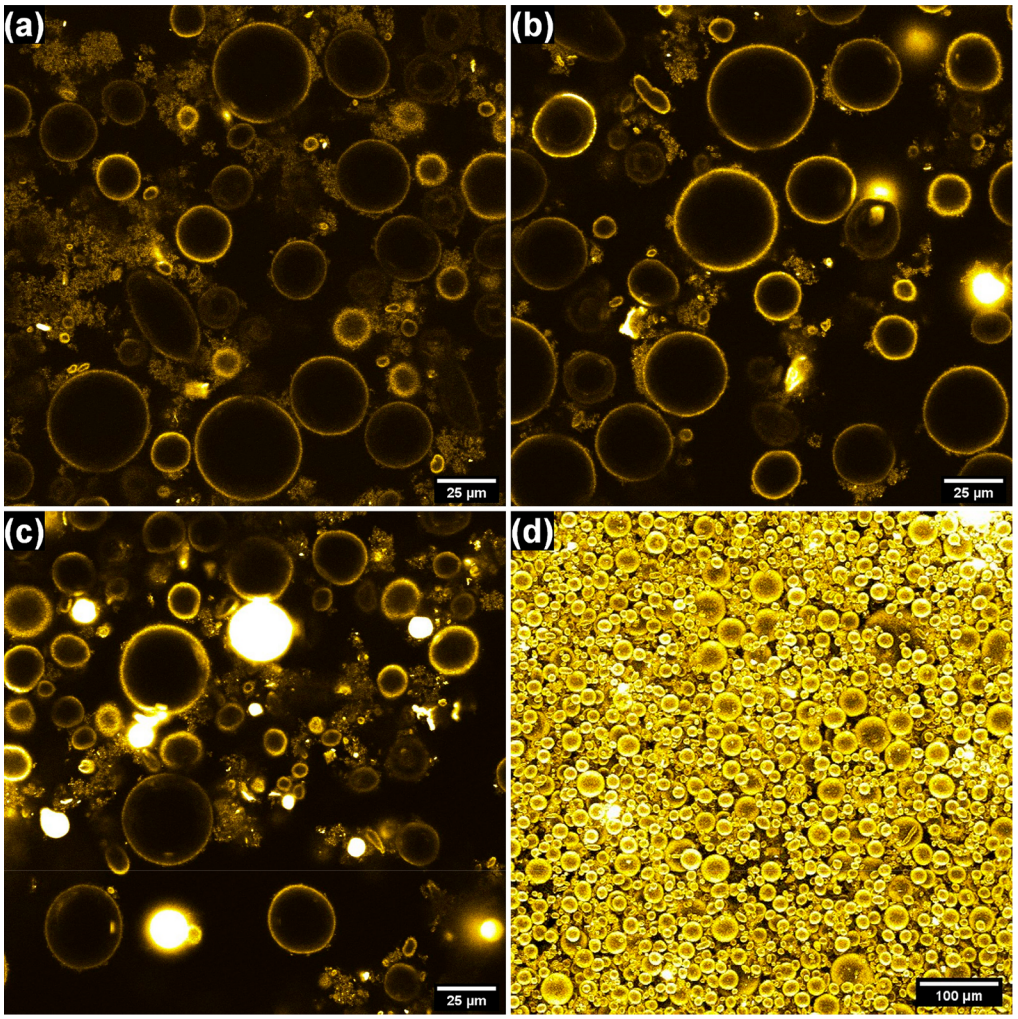

Figure 4. Confocal micrographs of capillary foams with a particle volume fraction ϕ_p = 0.92% of P_2 particles at different oil−particle ratios: ϱ = (a) 0.2, (b) 0.5, (c) 1. (d) *z*-Stack projection of lower magnification confocal micrographs (ϱ = 0.2).

c), more of the oil droplets are observed in the CF structure, and at ϱ = 1, the droplets are quite prevalent throughout the CF. Figure 3c shows that the excess of oil leads to a CF structure containing many oil droplets as well as a brighter oil−particle network consistent with larger capillary bridges.

While the increase in the number of droplets may be trivial, the presence and origin of droplets in the CFs is not. One potential reason why oil droplets were not observed in our previous work[20,22,24] could be that the oil−particle ratio used in that study was low ($\varrho \sim 0.14$). However, when the oil−particle ratio used to make CFs with P_1 here is reduced considerably (ϱ = 0.05), we still typically observe at least one droplet per field of view, and micrographs covering a larger area typically show several oil droplets present throughout the foam microstructure (see Figure S1). Another plausible reason for the presence of oil droplets in the CF microstructure is that the energy input supplied to the system in the frothing process may have been insufficient to finely distribute the remaining oil across the nascent particle network and bubble surfaces. Previous work on CFs has shown that the gel network has to be formed first before bubbles can be retained in the system.[22] The mixing energy has been observed to have a significant impact on the mechanical properties of the gel network in capillary suspensions and as such could also play a role in influencing the structure observed in CFs.[28] Effective production of CFs used in this work required frothing at the maximum speed of the homogenizing mixer, therefore the effect of mixing energy was not further explored. Apart from the amount of oil and the mixing energy, particle wettability may also determine the location of the oil in the CFs microstructure. Specifically, one might expect that oil droplets will not be accommodated when particles are preferentially wetted by the oil (poor o/w-emulsion stabilizers).

3.1.2. Effect of Particle Wettability on Capillary Foam Structure. Capillary foams, just like capillary suspensions, can be produced regardless of which liquid preferentially wets the particles (the continuous phase or secondary liquid). The particles' wetting preference does, however, determine the type of interparticle bridging (pendular bridges vs capillary aggregates) that drives gelation and yields, outside the foam bubbles, a capillary suspension in either the pendular or the capillary state.[16,18] Although the particles and oil bridges in our CFs are so small that we cannot directly see the exact type of bridging present in the confocal images of both Figures 2 and 3, we do know, from our emulsion tests, that our P_1 particles are preferentially wetted by water, because they stabilize a water-continuous emulsion upon mixing equal volumes of the aqueous dispersion and the oil (Table 1). For this reason, we believe that the hazy illuminated background seen outside the foam bubbles in Figures 2 and 3 originates from the oil bridges

https://doi.org/10.1021/acs.langmuir.1c01479
Langmuir 2021, 37, 10510−10520

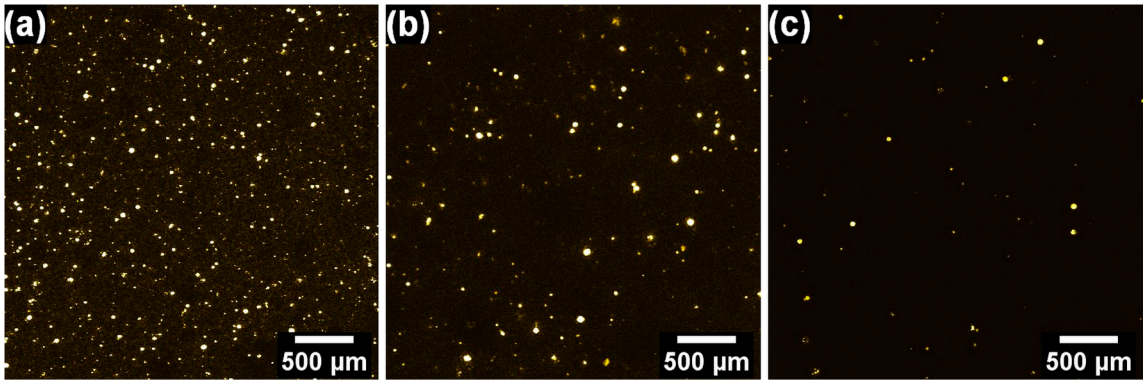

Figure 5. Low magnification confocal micrographs of capillary foams formed from (a) P_1, (b) P_2, and (c) P_3 particles at an oil−particle ratio $\varrho = 0.2$ and particle volume fraction $\phi_p = 0.92\%$.

in the capillary aggregates familiar from capillary suspensions with particles preferentially wetted by the liquid medium. The liquid bridges in the capillary state can be larger and more polydisperse than the pendular bridges, which wet the particles preferentially.[18]

In order to explore foams in the pendular state we turn to our more hydrophobic P_2 particles, which are known to be preferentially wetted by the oil (TMPTMA), since they stabilize oil-continuous emulsions of equal liquid volumes (Table 1). Figure 4 shows confocal images of CFs produced with P_2 particles at a volume fraction $\phi_p = 0.92\%$, and different oil−particle volume ratios (ϱ = 0.2, 0.5, 1). The first feature distinguishing Figures 4a−c from their counterparts in Figure 3 is the absence of a diffuse fluorescence signal from much of the space outside the oil coated bubbles. Although the diffuse signal was previously attributed to the oil−particle network in the capillary state, the absence of this signal does not imply the absence of a network in the present case. Instead, we conjecture that the oil−particle network in the pendular state fails to "light up" because the pendular bridges between the particle pairs are too small to yield a significant fluorescence signal, making the observation of the network in confocal imaging difficult. The images in Figure 4 also illustrate that, overall, there are significantly fewer oil droplets present in these pendular state foams compared to their capillary state counterparts in Figure 3, and again the prevalence of these droplets increases with the oil−particle ratio ϱ (Figure 4a−c). While Figure 4a could raise doubts whether any droplets are present at $\varrho = 0.2$, the zoomed-out z-stack projection of Figure 4d clearly shows a few oil droplets interspersed between the oil coated bubbles. These droplets are smaller in size and concentration than those seen in the corresponding image of the foam made with the hydrophilic P_1 particles (see Figure 2b); this shift in size and number of oil droplets supports our hypothesis that particle wettability contributes to the presence of oil droplets in CFs. We also note in passing that the CF bubbles obtained with P_2 particles, in many cases, appear closer to each other than the bubbles obtained with P_1 particles, an observation likely linked to the differences between the intervening particle networks as well.

To further illustrate the effects of particle wettability, we compare, in Figure 5a−c, more zoomed out confocal images of CFs prepared with the three particle types P_1−P_3 in order of increasing particle hydrophobicity. We note that the most hydrophobic particles (P_3) were found to also stabilize Pickering foams with excellent foamability and foam stability even in the absence of oil. The capillary foams shown in Figure 5, however, were prepared with a (condensed phase) volume fraction $\phi_p = 0.92\%$ of the respective particles and an oil−particle volume ratio $\varrho = 0.2$. The confocal images in Figure 5 indicate that the prevalence of oil droplets in CFs decreases with increasing particle hydrophobicity and reveals that even in the system with the most hydrophobic particles, oil droplets can still be found, albeit at low concentration.

The oily bubble coats cannot be seen in the images of Figure 5 because of their low magnification. At higher magnification of the confocal images (see Figure S3 in the Supporting Information), we observe that the foam bubbles are indeed coated with oil in all three cases, including the one where particles (P_3) are hydrophobic enough to stabilize a Pickering foam in the absence of oil. The images in Figures 3, 4, 5, and S3 show that the capillary foam microstructure changes with particle wettability and confirm that particle wettability influences the number of oil droplets incorporated in the CF at a given oil concentration.

3.2. Foam Rheology. The interactions within CFs give rise to mechanical foam properties that can be probed using rheometry. In prior work, we conducted extensive rheological studies on a CF containing large micron sized particles in a pendular state network.[23] In the following, we will investigate the rheological similarities and differences that exist between CFs with different particle network states and relate our findings to rheological differences reported for capillary suspensions in the corresponding states. We will also examine how the oil and particle content influence CF rheology.

We conducted frequency sweep (FS) and controlled shear stress (CSS) experiments to probe the rheology of CFs prepared from P_1 particles at different particle volume fractions and oil−particle ratios. The plateau of the storage modulus (referred to as the "plateau modulus" G_0 from here on) and yield stress (σ_y) of the CFs were obtained from the results of the respective FS and CSS experiments. The storage modulus (G') is a measure of the elasticity and provides an indication of the material rigidity. The plateau modulus in CFs is obtained in frequency sweeps by averaging the flat portions of the storage modulus plot (see Figure S5b). The yield stress on the other hand measures the resistance to flow in a material. The concept of yield stress in complex fluids is still a debated topic,[29] but for the purposes of this work, we shall define σ_y as the stress at which the transition from a nonsteady-state to a steady-state shear rate is observed (see Figure S5c).[30] Figure 6a shows the plot of the plateau modulus and the yield-stress

https://doi.org/10.1021/acs.langmuir.1c01479
Langmuir 2021, 37, 10510−10520

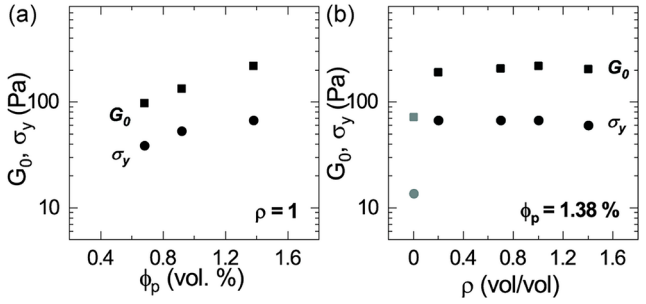

Figure 6. Plots of rheological changes to the plateau modulus (G_0: black squares) and yield stress (σ_y: black circles) in the capillary state, when (a) the particle volume fraction is varied at a fixed oil−particle ratio (ϱ) and (b) the oil−particle ratio is varied at a fixed particle fraction (ϕ_p) of P_1 particles. Gray markers in part b are for an oil-free foam (Pickering foam).

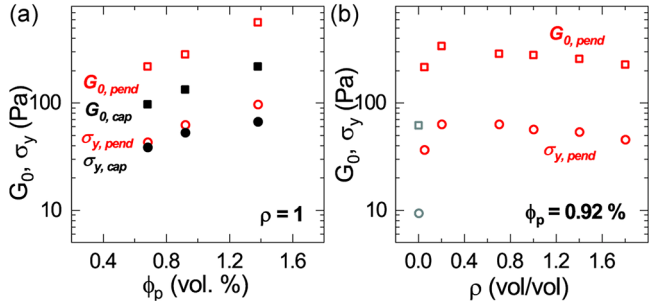

Figure 7. (a) Comparison of plateau modulus (G_0: squares) and yield stress (σ_y: circles) of capillary foams made with P_1 particles (solid symbols: capillary state) and P_2 particles (open symbols: pendular state). (b) Plot of the modulus (squares) and yield stress (circles) in CFs made from P_2 particles at varying oil−particle ratio when ϕ_p = 0.92%. Gray markers in part b are for the oil-free Pickering foam. Inserting data for the capillary state in part b for a direct comparison would compromise the clarity of the figure, but such comparative data can be found in Figure S6a.

for CFs made from P_1 particles when the particle volume fraction ϕ_p is varied at fixed oil−particle ratio ϱ = 1. The figure shows that the value of G_0 is higher than the value of σ_y; however both G_0 and σ_y increase with ϕ_p, indicating that the particle network strength in CFs increases with the particle fraction.

In Figure 6b, we plot the change in modulus and yield stress of CFs prepared with P_1 particles at different oil−particle ratios for ϕ_p = 1.38. The data shows that above some minimum threshold value of ϱ both G_0 and σ_y are insensitive to variations in the oil−particle ratio (and by extension, insensitive to the number of oil droplets in the oil regime explored). This insensitivity of G_0 and σ_y was established for different values of ϕ_p (see Figure S5a). The only significant change observed in Figure 6b is the increase in the values of G_0 and σ_y between ϱ = 0 and 0.2. This increase in G_0 and σ_y highlights the rheological differences between the Pickering foam (no oil, ϱ = 0) and the CF formed in the presence of a small amount of oil. Although we observe that the tiny amount of oil induces sharp rheological changes at different values of ϕ_p used to prepare the CFs, we note that the changes are more prominent as ϕ_p increases. Figure 6b shows that once the CF is formed, increasing ϱ to as much as 1.4 does not affect the rheological properties of the CF. In fact, the raw data of the FS and flow curves, from which the values of G_0 and σ_y in Figure 6b were extracted, collapse onto each other, showing that both the values of G_0 and σ_y are independent of ϱ for a given value of ϕ_p (see Figure S5b and c).

3.2.1. Effect of Particle Wettability on Capillary Foam Rheology. Apart from the changes in the microstructure of CFs, we observed that the particle wettability also affects the rheology of CFs. To show the effects of particle wettability on CF rheology, we compare the values of σ_y and G_0, in Figure 7a, that are obtained when the particle volume fraction is varied in CFs made from either P_1 particles (capillary state) or P_2 particles (pendular state).

The plot shows that CFs in the pendular state have higher values for both σ_y and G_0 in comparison to CFs in the capillary state. The modulus values of the CFs in the pendular state are almost double the values of the moduli in the capillary state ($G_{0,pend} \sim 2G_{0,cap}$), while the yield stress of the CFs, although more similar in both states, are still higher in the pendular state. The observation that the pendular state is associated with a higher network strength than the capillary state may be rationalized by noting that the network-strengthening inter-particle force mediated by the oil bridges contains two contributions: a contribution from the meniscus interfacial tension that is always attractive between two particles of equal wettability, and a contribution from the Laplace pressure that is also attractive in the case of concave bridges (pendular state) but repulsive in the case of convex bridges (capillary state). For a more quantitative description, we refer to the excellent historical perspective article by Danov et al.[31]

When we vary the oil−particle ratio between $0 \leq \varrho \leq 1.8$, keeping volume fraction of P_2 constant at ϕ_p = 0.92 vol %, we observe that both σ_y and G_0 increase initially for $0 \leq \varrho \leq 0.2$, peak at ϱ = 0.2, and then slightly decrease beyond $\varrho > 0.2$ (see Figure 7b). The rheology data on CFs in the pendular state bolsters our initial observation that increasing the oil concentration, over a wide range of oil−particle ratios, has little effect on the rheological properties of CFs. We expect however that, at very high concentrations of oil, there will be significant decreases in σ_y and G_0 of CFs as the strength of the oil bridges between the particles weaken due to the presence of large oil droplets disturbing the continuity of the particle network. It is also worth noting that the CFs made from P_3 produced the highest G_0 and σ_y, of all the particles used in this work (see Figure S8); this confirms the dual effect of the particle wettability on the both the state of the particle network and the rheology of CFs. Our results show that the type of bridging in the particle network quantitatively affects the values of G_0 and σ_y but does not alter the qualitative dependence of rheological properties on the oil and particle concentrations.

The effect of the particle wettability on the values of G_0 and σ_y in CFs is not so surprising, as we have previously explained that the particle network significantly contributes to the rheology of CFs. Our results show that the gel network in CFs becomes stronger as the particle wettability shifts toward the secondary liquid. The increase in σ_y and G_0 values likely results from the observed differences in the foam microstructure. Bossler et al. showed that in capillary *suspensions*, the formation of pendular bridges leads to stronger gel network than the bridging of multiple particles typical of networks in the capillary state.[17] Yang et al. also observed a decrease in the storage modulus in capillary suspensions as the particles become less wetted by the minority liquid.[32] Shifting the particle wettability away from the secondary liquid precludes the formation of pairwise concave bridges between particles in

https://doi.org/10.1021/acs.langmuir.1c01479
Langmuir 2021, 37, 10510−10520

the gel network because the system energy is minimized by particles clustering around droplets of the secondary liquid. Although particle clusters are more prominent in the capillary state, Bindgen et al. observed that increasing the oil concentration also led to the occurrence of some particle clusters in pendular state networks.[33] That study established that the increase in particle clusters correlates with a reduced G_0 even in the pendular state of capillary suspensions. The results of Bindgen's work are consistent with the results of Bossler and Yang and shed light on the effects of wettability on particle clustering and the rheology of capillary suspensions.

In capillary foams the rheological differences between the pendular and capillary network states are less pronounced than in capillary suspensions. In capillary suspension, the values of G_0 and σ_y are hundreds to thousands of Pascals lower in the capillary state than in the pendular state.[34] By comparison, the values of G_0 and σ_y in both states in CFs only differ by tens to hundreds of Pascals. This significant reduction in the effect of particle wettability on the rheology stems from the presence of bubbles in CFs and the fact that the particle network occupies a lower volume fraction in CFs than in capillary suspensions. Although we know that the bubbles and the particle network both contribute to CF rheology, their contributions are difficult to separate. Another reason capillary suspension rheology depends sensitively on the network type is because the network dictates how the secondary liquid is incorporated into the network. The rheology of capillary suspensions is sensitive to excess secondary liquid, which has been shown to weaken the network strength. Capillary foams, by contrast, are less sensitive to weakening by excess oil, because here the oil can be partly sequestered in the bubble coats where it does not hurt the network strength.

The micrographs in Figures 2, 3, and 4 show that the presence of oil droplets in CFs depends on the particle wettability and is a function of ϱ. We note, however, that the droplets of excess oil do not have a significant effect on the plateau modulus and yield stress: at a fixed particle wettability, both properties hardly change with ϱ. In both network types, the oil in CFs primarily coats the bubbles and bridges the particles and only exists secondarily as droplets in the particle network. Although the number of droplets and the droplet sizes increase with the oil concentration, the overall oil content never exceeds 3% of the CF volume, and as such the oil droplets do not significantly contribute to the CF rheology. We believe that the effects of oil saturation on CF rheology are mitigated by the dominance of the capillary forces exerted by the bubbles and the particle network, both of which are connected and occupy a larger volume fraction than the droplets.

3.3. Foamability. The particle network in CFs is intimately connected to the foam rheology as seen above, but also responsible for the retention of air bubbles within the foam.[22] Foamability in CFs depends on the formation of oil-bridges between the particles and particle-assisted spreading of oil around gas bubbles. Therefore, we studied how the network type and oil content affect the total amount of air retained and its volume fraction in the resulting foam. Here, we prepared CFs at different volume fractions of particles with different wettability while keeping ϱ constant, and at different oil−particle ratios while keeping ϕ_p constant. The foam volume and the gas volume fraction ("foam quality") of the CFs produced were quantified to understand the effects of ϕ_p, ϱ, and wettability on foamability. We determined the foam volume by measuring the height of the foam head in a cylindrical vial with known radius. The foam quality ϕ_g was determined according to eq 2.

$$\phi_g = \frac{\text{foam volume} - \text{volume of (particle suspension + oil)}}{\text{foam volume}} \tag{2}$$

Once the CFs were prepared, the foam volume and quality were monitored for 2 h; no significant changes with time were observed following the first hour, we therefore consider and call the foam volume at this stage "final". Figures 8a and b show the values of the initial foam volume and final foam quality of CFs in the pendular and capillary states when ϕ_p is varied at a constant oil−particle ratio of ϱ = 1.

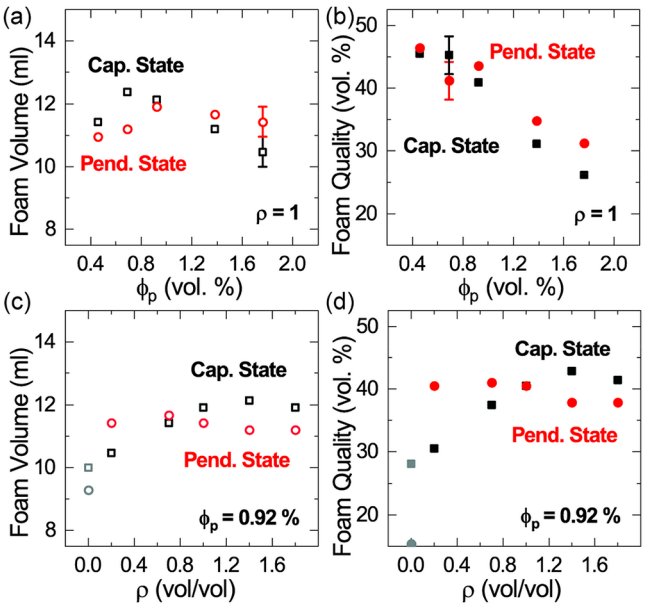

Figure 8. Plots of (a) capillary foam volume and (b) foam quality as a function of particle volume fraction (ϕ_p). Plots of (c) capillary foam volume and (d) foam quality as a function of oil−particle ratio (ϱ). The estimated typical uncertainty, indicated for just a few representative data points, results primarily from accuracy limitations in measuring the foam height.

Figure 8a shows that the values of the initial foam volumes of CFs in both network states follow a similar trend; both values of the foam volume initially increase with ϕ_p and then decrease at higher values of ϕ_p. We note, however, that the maxima for the initial foam volume plots are different; while the initial foam volume in the capillary state starts to decrease at $\phi_p \approx 0.7$ vol %, the initial foam volume in the pendular state does not start to decrease until $\phi_p \approx 1$ vol % and does not decrease as much as the foam volume in capillary state. The plots of initial foam quality for both states follow the same nonmonotonic trend as the plots of the initial foam volume (Figures S9 and S10): the initial foam quality increases with ϕ_p and then decreases as ϕ_p increases further. Figure 8b highlights the *final* foam quality obtained after 2 h. This final foam quality decreases monotonically as a function of ϕ_p for foams both in the pendular and in capillary states.

The observed dependence of rheological properties like G_0 on ϕ_p can help explain some of the foamability results in CFs. The CF volume and quality plots reveal that the initial foam volume is determined by the volume of gas incorporated into

https://doi.org/10.1021/acs.langmuir.1c01479
Langmuir 2021, 37, 10510−10520

the foam matrix and is connected to the strength of the gel network entrapping the gas bubbles. To entrap gas in a viscoelastic medium, the bubbles need to be generated via frothing, and immobilized within the medium. We suspect that the strength of the medium works against bubble generation, since generating a bubble requires major deformation of the medium. As ϕ_p increases, rigidity in the particle network increases, thus making bubble generation more challenging in CFs. Figure 8b shows that the volume of gas incorporated into CFs linearly decreases with increasing ϕ_p, which correlates with an increase in G_0, and leads us to suggest that the strength of the particle network plays a role in determining the volume of air incorporated into the CF. As previously reported for ternary fluid/fluid/particle systems, where one of the fluids is air, the system "decides" how much air is entrained.[8] While the bubble interface in ternary systems is stabilized solely by particles, CFs additionally require oil to coat the bubbles.

In Figures 8c and d, we show the initial foam volume and final foam quality plots for CFs produced when varying ϱ at constant ϕ_p = 0.92 vol %. The foam volume and foam quality plots in the capillary state show that an initial increase in ϱ results in an increase in both initial foam volume and final foam quality. In the pendular state, however, the foam volume and quality of the CFs formed is insensitive to the oil content for $\varrho \geq 0.2$. It is important to note that when increasing ϱ the oil volume added to the mixture used to prepare the CFs does not account for the increase in CF volume observed in Figure 8c. In fact, the total increase in the oil concentration is ~100 μL, whereas the volume increase is several milliliters. Moreover, the addition of a miniscule amount of oil (~12 μL), to increase ϱ from 0 to 0.2, not only enables the creation of a capillary foam rather than a Pickering foam (oil-free, particle stabilized foam) but also leads to a considerable increase (>10 vol %) in the volume of gas incorporated into the CF matrix; see Figure 8c. We also observe that the range of gas fractions ($0.3 \leq \phi_g \leq 0.45$) obtained from volumetric analysis in eq 2 closely agree with the fraction of bubbles estimated from the confocal micrographs. For example, confocal micrographs in Figures 3a and 4a suggest that the foam quality of CFs, at ϱ = 0.2, is higher in the pendular state than in the capillary state. The values in Figure 8d, at ϱ = 0.2, confirm that the foam quality in the pendular state at ~40% is higher than the foam quality in the capillary state at ~30%. Given the trends observed in how the foam volume, foam quality, and microstructure change with ϱ for both pendular and capillary states (see Figures 3, 4, 8c, and 8d), we better understand how the bubbles in CFs can act as reservoir for oil. When the oil content of a CF in the capillary state is increased, that oil can go toward the bubble coats, but the particle network can also absorb more oil, forming more large bridges connecting multiple particles; it can more readily accommodate droplets of bulk oil (bright spots in micrographs) because the particles have the right wettability to stabilize O/W emulsion droplets. In contrast, the oil content in the particle network of pendular state CFs does not easily grow by incorporating large oil bridges or particle-stabilized droplets. Rather, the excess oil in pendular state foams goes primarily into bubble coats, and the foam volume and quality are insensitive to the oil content.

3.4. Short-Term Foam Stability. The volume of CFs was measured at different time points within the 2 h experimental time to determine the relative foam volume changes and thereby quantify the short-term stability of the prepared CFs at different particle volume fractions and oil−particle ratios. In Figures 9a and b, we plot the volume evolution of foams in the capillary state (normalized by their respective initial values shown in Figures 8a and c). The same qualitative trends in the foam evolution with varying ϕ_p and ϱ seen in Figure 9 were also found in pendular state foams (see Figure S11a). The loss of volume monitored here is primarily due to water drainage from the foam head.

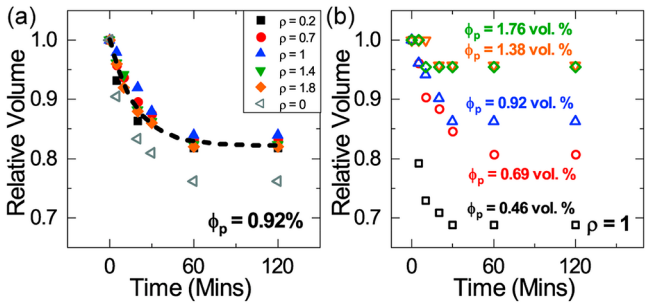

Figure 9. Plot of relative volume change with time in CFs prepared with P_1 particles (capillary state) when the (a) oil−particle ratio (ϱ) and (b) particle volume fraction (ϕ_p) are varied. Data for the Pickering foam (ϱ = 0) in part a are depicted as gray open markers.

Inspection of both plots in Figure 9 shows that ϕ_p has a stronger influence than ϱ on the change in the volume of CFs. In fact, a closer look at Figure 9a shows that foam stability is essentially independent of ϱ as long as a minimum amount of oil is present. All the data for CFs at different nonzero oil−particle ratios follow a similar trend and fall onto a single curve. We found that the master curve for the CF stability at this ϕ_p can be expressed by an exponential foam decay from the initial volume V_o to the final volume V_∞; i.e., the relative volume follows $\frac{V(t)}{V_o} = \frac{V_\infty}{V_o} + \left(1 - \frac{V_\infty}{V_o}\right)e^{-t/\tau}$ with a characteristic decay time τ = 19 min for the capillary state (dashed line in Figure 9a) and τ = 7.0 min for the pendular state. In a similar experiment where ϱ was varied at ϕ_p = 1.38 vol %, we also found that ϱ had no effect on the relative volume change in time and, by extension, on the stability of the CFs at that particle volume fraction (see Figure S11b). We should also point out that the relative volume change with time for the Pickering foam (ϱ = 0) does not fall onto the master curve (see open triangles in Figure 9a). This highlights a stability difference between capillary foams and Pickering foams and shows that the presence of even a little bit of oil impacts foam stability in this system.

Figure 9b shows that the particle volume fraction (ϕ_p) strongly affects the stability of CFs in time. The plots show that the retained foam volume increases with the particle volume fraction in the CF. We note that even at the highest volume fraction of particles tested, ϕ_p = 1.76 vol %, the foam volume still decreases slightly with time. The data in Figure 9b also suggests two stability regimes: for ϕ_p < 1.38 vol %, the foam stability over time is sensitive to changes in ϕ_p, whereas for $\phi_p \geq$ 1.38 the foam stability becomes insensitive to ϕ_p.

The strength of the particle network also influences the stability of CFs over time. Figure 9b shows that drainage over time in CFs reduces as ϕ_p increases. Strengthening the particle network, by increasing ϕ_p, arrests and significantly reduces drainage in CFs. We suspect that as network strength increases, more bubbles and particles are connected and held tightly

https://doi.org/10.1021/acs.langmuir.1c01479
Langmuir 2021, 37, 10510−10520

within the CF network. We see that once the foam is formed, a stronger medium favors foam stability.

In summary, we have seen that although the particle network in CFs is mediated by both the oil and particles, it is the particle volume fraction and not the volume of oil that mostly controls the network strength in CFs (Figures 6 and 7). The particle network strength influences the volume of air generated and retained in CFs (Figures 8b and 9b). At low network strength it is easy to generate bubbles, but foam stability is poor because of the lower gel strength of the medium. In contrast, CF stability increases with network strength whereas foamability decreases because the medium is not easily deformed at high network strength. Furthermore, we have seen that both G_0 and foam stability in CFs are insensitive to the volume of oil at constant ϕ_p (Figures 6b and 9a) and that, without the oil, G_0 decreases and the Pickering foam produced is less stable than the CF. The finding that ϕ_p mainly controls the modulus in CFs is in stark contrast to what has been observed in previous research on capillary suspensions, the gas-free analogues of our CFs.[16,35] It has been shown that increasing ϕ_p results in a higher modulus (G) in capillary suspensions.[28,36] Increasing ϱ from 0 to 0.2, increases G; however, for $\varrho > 0.2$, the value of G decreases for capillary suspensions in the pendular state. The work on capillary suspensions points to the fact that the maximum strength of the gel particle network is achieved around $\varrho \cong 0.2$ and that further addition of secondary liquid beyond this point is detrimental to the strength of the particle network.[33,35] In CFs, by contrast, the additional secondary liquid (excess oil) hardly affects the network strength but can be beneficial to foamability. CF volume and quality in the capillary state increase with ϱ (Figures 8c and d), whereas both G_0 and σ_y are insensitive to ϱ. We thus find that foamability in CFs is determined by both ϕ_p and ϱ. Our data suggests that additional oil helps to stabilize newly formed bubbles, thereby increasing the volume of gas incorporated into CFs. Furthermore, we see that the excess oil does not significantly affect the rheology and stability of CFs and can promote foamability.

4. CONCLUSIONS

We have investigated how varying the wettability and concentrations of oil and particles in capillary foams (CFs) can influence properties such as the microstructure and rheology of CFs. By performing microscopy, rheology, and foaming experiments, we were able to determine how the structure of the particle network, the size of the foam head, and the rheological properties of yield stress and storage modulus in CFs depend on the volume fraction of particles, the concentration of oil, and the particle wettability.

Confocal microscopy images of CFs highlight the foam's microstructure and document, for the first time, the inclusion of oil droplets in CFs. We observe that the particle wettability influences the rheology and the presence of droplets in the CF microstructure. Our rheology results show that particle volume fraction (ϕ_p) controls gel strength in CFs. We see that both the yield stress (σ_y) and plateau modulus (G_0) in CFs are primarily controlled by ϕ_p and rather insensitive to the oil concentration because much of the excess oil in CFs can partition into the bubble coats. Consequently, the foam stability, which correlates with the gel strength, is also fairly insensitive to variations in the oil content but improves with increasing particle volume fraction. The dependencies for foamability by contrast are more complicated because the nascent gel network formed in the frothing process has the antagonistic effects of making bubble generation harder and bubble retention easier. These observations support the notion that the gel strength determines both foamability and stability in CFs, that CF properties are oil tolerant and can be tailored to meet specific application demands.

The results of this work not only extend our knowledge of CFs but also help to better understand how CFs differ from ternary systems and provide a starting point for developing new commercial foam products and engineering CFs for use in industrial processes, an example of which could be enhanced oil recovery.

■ ASSOCIATED CONTENT

Supporting Information

The Supporting Information is available free of charge at https://pubs.acs.org/doi/10.1021/acs.langmuir.1c01479.

Additional confocal micrographs of capillary foams as well as raw data from the rheology and foaming experiments (PDF)

■ AUTHOR INFORMATION

Corresponding Authors

Sven H. Behrens − *School of Chemical and Biomolecular Engineering, Georgia Institute of Technology, Atlanta, Georgia 30332, United States;* Present Address: Polymer Science & Materials Chemistry, Exponent Inc., Atlanta, Georgia 30326, United States; orcid.org/0000-0002-3528-4053; Email: sbehrens@exponent.com

J. Carson Meredith − *School of Chemical and Biomolecular Engineering, Georgia Institute of Technology, Atlanta, Georgia 30332, United States;* orcid.org/0000-0003-2519-5003; Email: carson.meredith@chbe.gatech.edu

Author

Omotola Okesanjo − *School of Chemical and Biomolecular Engineering, Georgia Institute of Technology, Atlanta, Georgia 30332, United States;* orcid.org/0000-0002-2123-6288

Complete contact information is available at: https://pubs.acs.org/10.1021/acs.langmuir.1c01479

Notes

The authors declare no competing financial interest.

■ ACKNOWLEDGMENTS

The work in this paper was made possible with the financial support from the National Science Foundation (CBET-1706475). We would also like to acknowledge the generous donation of silica particles from Wacker-Chemie (Germany) and Evonik (USA). We would like to thank A. Fernandez-Nieves for access to the rheometer in the GT Soft Condensed Matter Lab.

■ REFERENCES

(1) Nagarkar, S. P.; Velankar, S. S. Morphology and rheology of ternary fluid-fluid-solid systems. *Soft Matter* **2012**, *8* (32), 8464.

(2) Yang, J.; Roell, D.; Echavarria, M.; Velankar, S. S. A microstructure-composition map of a ternary liquid/liquid/particle system with partially-wetting particles. *Soft Matter* **2017**, *13* (45), 8579−8589.

(3) Amoabeng, D.; Tempalski, A.; Young, B. A.; Binks, B. P.; Velankar, S. S. Fumed silica induces co-continuity across a wide composition range in immiscible polymer blends. *Polymer* **2020**, *186*, 121831.
(4) Cai, D.; Clegg, P. S.; Li, T.; Rumble, K. A.; Tavacoli, J. W. Bijels formed by direct mixing. *Soft Matter* **2017**, *13* (28), 4824−4829.
(5) Tarimala, S.; Dai, L. L. Structure of Microparticles in Solid-Stabilized Emulsions. *Langmuir* **2004**, *20* (9), 3492−3494.
(6) Aussillous, P.; Quéré, D. Liquid marbles. *Nature* **2001**, *411* (6840), 924−927.
(7) Heidlebaugh, S. J.; Domenech, T.; Iasella, S. V.; Velankar, S. S. Aggregation and separation in ternary particle/oil/water systems with fully wettable particles. *Langmuir* **2014**, *30* (1), 63−74.
(8) Velankar, S. S. A non-equilibrium state diagram for liquid/fluid/particle mixtures. *Soft Matter* **2015**, *11* (43), 8393−403.
(9) Ramsden, W. Separation of solids in the surface-layers of solutions and 'Suspensions' (Observations on surface-membranes, bubbles, emulsions, and mechanical coagulation). Preliminary Account. *Proc. R. Soc. London* **1903**, *72* (479), 156−164.
(10) Pickering, S. U. Emulsions. *J. Chem. Soc., Trans.* **1907**, *91*, 2001−2021.
(11) Hunter, T. N.; Pugh, R. J.; Franks, G. V.; Jameson, G. J. The role of particles in stabilising foams and emulsions. *Adv. Colloid Interface Sci.* **2008**, *137* (2), 57−81.
(12) Tavacoli, J. W.; Thijssen, J. H. J.; Schofield, A. B.; Clegg, P. S. Novel, Robust, and Versatile Bijels of Nitromethane, Ethanediol, and Colloidal Silica: Capsules, Sub-Ten-Micrometer Domains, and Mechanical Properties. *Adv. Funct. Mater.* **2011**, *21* (11), 2020−2027.
(13) Yang, Y.; Fang, Z.; Chen, X.; Zhang, W.; Xie, Y.; Chen, Y.; Liu, Z.; Yuan, W. An Overview of Pickering Emulsions: Solid-Particle Materials, Classification, Morphology, and Applications. *Front. Pharmacol.* **2017**, *8*, 287.
(14) Koos, E. Capillary suspensions: Particle networks formed through the capillary force. *Curr. Opin. Colloid Interface Sci.* **2014**, *19* (6), 575−584.
(15) Butt, H. J. Materials science. Controlling the flow of suspensions. *Science* **2011**, *331* (6019), 868−9.
(16) Koos, E.; Willenbacher, N. Capillary Forces in Suspension Rheology. *Science* **2011**, *331* (6019), 897.
(17) Bossler, F.; Koos, E. Structure of Particle Networks in Capillary Suspensions with Wetting and Nonwetting Fluids. *Langmuir* **2016**, *32* (6), 1489−501.
(18) Koos, E.; Willenbacher, N. Particle configurations and gelation in capillary suspensions. *Soft Matter* **2012**, *8* (14), 3988.
(19) Mohraz, A. Interfacial routes to colloidal gelation. *Curr. Opin. Colloid Interface Sci.* **2016**, *25*, 89−97.
(20) Zhang, Y.; Wu, J.; Wang, H.; Meredith, J. C.; Behrens, S. H. Stabilization of liquid foams through the synergistic action of particles and an immiscible liquid. *Angew. Chem., Int. Ed.* **2014**, *53* (49), 13385−9.
(21) Behrens, S. H. Oil-coated bubbles in particle suspensions, capillary foams, and related opportunities in colloidal multiphase systems. *Curr. Opin. Colloid Interface Sci.* **2020**, *50*, 101384.
(22) Zhang, Y.; Wang, S.; Zhou, J.; Benz, G.; Tcheimou, S.; Zhao, R.; Behrens, S. H.; Meredith, J. C. Capillary Foams: Formation Stages and Effects of System Parameters. *Ind. Eng. Chem. Res.* **2017**, *56* (34), 9533−9540.
(23) Okesanjo, O.; Tennenbaum, M.; Fernandez-Nieves, A.; Meredith, J. C.; Behrens, S. H. Rheology of capillary foams. *Soft Matter* **2020**, *16* (29), 6725−6732.
(24) Zhang, Y.; Allen, M. C.; Zhao, R.; Deheyn, D. D.; Behrens, S. H.; Meredith, J. C. Capillary foams: stabilization and functionalization of porous liquids and solids. *Langmuir* **2015**, *31* (9), 2669−76.
(25) Dzuy, N. Q.; Boger, D. V. Direct Yield Stress Measurement with the Vane Method. *J. Rheol.* **1985**, *29* (3), 335−347.
(26) Salonen, A.; Lhermerout, R.; Rio, E.; Langevin, D.; Saint-Jalmes, A. Dual gas and oil dispersions in water: production and stability of foamulsion. *Soft Matter* **2012**, *8* (3), 699−706.
(27) Koczo, K.; Lobo, L. A.; Wasan, D. T. Effect of oil on foam stability: Aqueous foams stabilized by emulsions. *J. Colloid Interface Sci.* **1992**, *150* (2), 492−506.
(28) Bossler, F.; Weyrauch, L.; Schmidt, R.; Koos, E. Influence of mixing conditions on the rheological properties and structure of capillary suspensions. *Colloids Surf., A* **2017**, *518*, 85−97.
(29) Bonn, D.; Denn, M. M.; Berthier, L.; Divoux, T.; Manneville, S. Yield stress materials in soft condensed matter. *Rev. Mod. Phys.* **2017**, *89* (3), 035005.
(30) Da Cruz, F.; Chevoir, F.; Bonn, D.; Coussot, P. Viscosity bifurcation in granular materials, foams, and emulsions. *Phys. Rev. E: Stat. Phys., Plasmas, Fluids, Relat. Interdiscip. Top.* **2002**, *66* (5), 051305.
(31) Danov, K. D.; Georgiev, M. T.; Kralchevsky, P. A.; Radulova, G. M.; Gurkov, T. D.; Stoyanov, S. D.; Pelan, E. G. Hardening of particle/oil/water suspensions due to capillary bridges: Experimental yield stress and theoretical interpretation. *Adv. Colloid Interface Sci.* **2018**, *251*, 80−96.
(32) Yang, J.; Heinichen, N.; Velankar, S. S. The effect of particle wettability on the of rheology particulate suspensions with capillary force. *Colloids Surf., A* **2018**, *558*, 164−170.
(33) Bindgen, S.; Bossler, F.; Allard, J.; Koos, E. Connecting particle clustering and rheology in attractive particle networks. *Soft Matter* **2020**, *16* (36), 8380−8393.
(34) Bossler, F.; Maurath, J.; Dyhr, K.; Willenbacher, N.; Koos, E. Fractal approaches to characterize the structure of capillary suspensions using rheology and confocal microscopy. *J. Rheol.* **2018**, *62* (1), 183−196.
(35) Domenech, T.; Velankar, S. S. On the rheology of pendular gels and morphological developments in paste-like ternary systems based on capillary attraction. *Soft Matter* **2015**, *11* (8), 1500−16.
(36) Koos, E.; Kannowade, W.; Willenbacher, N. Restructuring and aging in a capillary suspension. *Rheol. Acta* **2014**, *53* (12), 947−957.

https://doi.org/10.1021/acs.langmuir.1c01479
Langmuir 2021, 37, 10510−10520